

Low-Temperature Photochemistry of $[\text{Fe}_2(\text{CO})_7(\text{L})]$ ($\text{L} = \text{bpy}$, phen) and $[\text{Fe}_2(\text{CO})_6(\text{L}')]$ ($\text{L}' = \text{R-PyCa}$, R-DAB) Complexes. Stabilization of $[\text{Fe}_2(\text{CO})_7(\text{R-PyCa})]$

Hans K. van Dijk, Derk J. Stufkens,* Ad Oskam, Marc Rotteveel, and Dick Heijdenrijk

Anorganisch Chemisch Laboratorium, University of Amsterdam, Nwe. Achtergracht 166,
1018 WV Amsterdam, The Netherlands

Received December 15, 1986

The low-temperature photochemistry of $[\text{Fe}_2(\text{CO})_7(\text{L})]$ ($\text{L} = 2,2'$ -bipyridine (bpy), 1,10-phenanthroline (phen)) and $[\text{Fe}_2(\text{CO})_6(\text{L}')]$ ($\text{L}' = \text{pyridine-2-carbaldehyde imine (R-PyCa)}$, 1,4-diaza-1,3-butadiene (R-DAB)) complexes in 2-MeTHF is described. Irradiation of the $[\text{Fe}_2(\text{CO})_7(\text{L})]$ complexes into the low-energy MLCT band causes the substitution of CO by nucleophiles, such as phosphines and N-donor ligands. The structures of the photoproducts appear to depend on the electronic properties of the substituting ligand. The crystal structure of one such a photoproduct, viz., the complex $[\text{Fe}_2(\text{CO})_6(\text{bpy})(\text{P}(n\text{-Bu})_3)]$ has been determined. The crystals are triclinic, space group $P\bar{1}$, with $a = 10.727(1) \text{ \AA}$, $b = 14.517(2) \text{ \AA}$, $c = 10.306(2) \text{ \AA}$, $\alpha = 97.30(1)^\circ$, $\beta = 96.53(1)^\circ$, $\gamma = 74.13(2)^\circ$, $V = 1525.9(7) \text{ \AA}^3$, and $Z = 2$. A total of 2425 intensities above the $3\sigma(I)$ level were used to refine the structure to a final R value of 0.057. The Fe-C bond trans to the phosphine ligand in this complex (2.244 (6) \AA) is shorter than the corresponding bond in the parent compound $[\text{Fe}_2(\text{CO})_7(\text{bpy})]$. The substitution of CO by a phosphine ligand has hardly any influence on the Fe-Fe bond length, which is 2.6048 (14) \AA in this complex and 2.611 \AA in $[\text{Fe}_2(\text{CO})_7(\text{bpy})]$. The $[\text{Fe}_2(\text{CO})_6(\text{R-PyCa})]$ complexes do not show release of CO but instead show a change of coordination of the R-PyCa ligand from $\sigma\text{-N}$, $\mu\text{-N}'$, $\eta^2\text{-CN}'$ (6e) into $\sigma\text{-N}$, $\sigma\text{-N}'$ (4e) upon irradiation of a 133 K solution in 2-MeTHF at 488 nm. When the temperature of the solution with the photoproduct is raised to 173 K in the presence of free CO, $[\text{Fe}_2(\text{CO})_7(\text{R-PyCa})]$ complexes are formed, which have the same structure as $[\text{Fe}_2(\text{CO})_7(\text{L})]$ ($\text{L} = \text{bpy}$, phen) and are stable up to 260 K. The $[\text{Fe}_2(\text{CO})_6(\text{R-DAB})]$ complexes show a similar change in coordination of the DAB ligand, which is however accompanied here by release of CO.

Introduction

Low-valence transition-metal complexes of α -diimine ligands are highly colored because of the presence of low-energy metal to α -diimine charge-transfer (MLCT) transitions. For a series of d^6 $[\text{M}(\text{CO})_4(\alpha\text{-diimine})]$ ($\text{M} = \text{Cr}$, Mo, W) and d^8 $[\text{M}'(\text{CO})_3(\alpha\text{-diimine})]$ ($\text{M}' = \text{Fe}$, Ru) complexes we have studied the spectroscopic and photochemical properties and we have found a close relationship between the photochemistry and resonance Raman (rR) spectra of these complexes.¹⁻¹⁰

Recently, this work has been extended to the binuclear complexes $[(\text{CO})_5\text{MM}'(\text{CO})_3(\alpha\text{-diimine})]$ ¹¹⁻¹⁵ ($\text{M}, \text{M}' = \text{Mn}$,

Re) and $[\text{Ph}_3\text{SnM}'(\text{CO})_3(\alpha\text{-diimine})]$ ($\text{M}' = \text{Mn}$, Re)¹⁶ in order to study the influence of MLCT excitation on the metal-metal bond. In all these complexes the α -diimine ligands used, 2,2'-bipyridine (bpy), 1,10-phenanthroline (phen), pyridine-2-carbaldehyde imine (R-PyCa; $\text{C}_5\text{H}_4\text{NCH}=\text{NR}$),¹⁷ and 1,4-diaza-1,3-butadiene (R-DAB; $\text{RN}=\text{CHCH}=\text{NR}$),¹⁷ are $\sigma\text{-N}$, $\sigma\text{-N}'$ (4e) coordinated to one metal atom, and their complexes show similar photochemical reactions. In the corresponding binuclear iron carbonyl complexes, however, the coordination mode of the α -diimine ligands depends on the ligand used. Thus in $[\text{Fe}_2(\text{CO})_7(\text{L})]$ ($\text{L} = \text{bpy}$, phen) the ligand L is again $\sigma\text{-N}$, $\sigma\text{-N}'$ coordinated to one of the Fe atoms (see Figure 1a). The molecular structure of these complexes, which has been determined by Cotton and co-workers,¹⁸ clearly shows the presence of a symmetrical bridging carbonyl ("real" bridge) and a semibridging one. This paper describes the photochemistry of these complexes in the presence of different kinds of nucleophilic ligands. The crystal structure of one of the photoproducts, viz., $[\text{Fe}_2(\text{CO})_6(\text{bpy})(\text{P}(n\text{-Bu})_3)]$, is presented and used for the interpretation of the results.

For the corresponding R-PyCa and R-DAB ligands the complexes $[\text{Fe}_2(\text{CO})_6(\text{L}')]$ ($\text{L}' = \text{R-PyCa}$, R-DAB) are found

(1) Balk, R. W.; Stufkens, D. J.; Oskam, A. *Inorg. Chim. Acta* 1978, 28, 133.

(2) Balk, R. W.; Stufkens, D. J.; Oskam, A. *Inorg. Chim. Acta* 1979, 34, 267.

(3) Balk, R. W.; Stufkens, D. J.; Oskam, A. *J. Chem. Soc., Dalton Trans.* 1982, 275.

(4) Balk, R. W.; Stufkens, D. J.; Oskam, A. *J. Chem. Soc., Dalton Trans.* 1981, 1124.

(5) Staal, L. H.; Stufkens, D. J.; Oskam, A. *Inorg. Chim. Acta* 1978, 26, 255.

(6) Balk, R. W.; Snoeck, T.; Stufkens, D. J.; Oskam, A. *Inorg. Chem.* 1980, 19, 3015.

(7) Kokkes, M. W.; Stufkens, D. J.; Oskam, A. *J. Chem. Soc., Dalton Trans.* 1983, 439.

(8) Kokkes, M. W.; Stufkens, D. J.; Oskam, A. *J. Chem. Soc. Dalton Trans.* 1984, 1005.

(9) Servaas, P. C.; van Dijk, H. K.; Snoeck, T. L.; Stufkens, D. J.; Oskam, A. *Inorg. Chem.* 1985, 24, 4494.

(10) van Dijk, H. K.; Servaas, P. C.; Stufkens, D. J.; Oskam, A. *Inorg. Chim. Acta* 1985, 179-183.

(11) Kokkes, M. W.; Snoeck, T. L.; Stufkens, D. J.; Oskam, A.; Christophersen, M.; Stam, C. H. *J. Mol. Struct.* 1985, 131, 11-29.

(12) Kokkes, M. W.; Stufkens, D. J.; Oskam, A. *Inorg. Chem.* 1985, 24, 293.

(13) Kokkes, M. W.; Stufkens, D. J.; Oskam, A. *Inorg. Chem.* 1985, 24, 4411.

(14) Kokkes, M. W.; de Lange, W. G. J.; Stufkens, D. J.; Oskam, A. *J. Organomet. Chem.* 1985, 294, 59.

(15) Stufkens, D. J.; Oskam, A.; Kokkes, M. W. *ACS Symp. Ser.* 1986, No. 307, 66.

(16) Andr ea, R. R.; Stufkens, D. J.; Oskam, A. to be submitted for publication.

(17) Most R-PyCa and R-DAB molecules have the general formula $\text{C}_5\text{H}_4\text{NCR}'=\text{NR}$ and $\text{RN}=\text{CR}'-\text{CR}''=\text{NR}$, respectively. Usually however, the substituents R' and R'' are protons and the abbreviations R-PyCa and R-DAB are used for this important subgroup. For the rarely encountered ligands $\text{C}_5\text{H}_4\text{NCR}'=\text{NR}$ and $\text{RN}=\text{CR}'\text{CR}''=\text{NR}$ (R' and $\text{R}'' \neq \text{H}$) the abbreviations R-PyCa $\{\text{R}'\}$ and R-DAB $\{\text{R}', \text{R}''\}$ are used. See also: van Koten, G.; Vrieze, K. *Adv. Organomet. Chem.* 1982, 21, 151.

(18) Cotton, F. A.; Troup, J. M. *J. Am. Chem. Soc.* 1974, 96, 123.

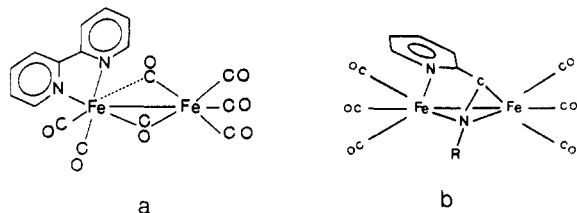


Figure 1. Structures of $[\text{Fe}_2(\text{CO})_7(\text{bpy})]$ (a) and $[\text{Fe}_2(\text{CO})_6(\text{R-PyCa})]$ (b).

as stable compounds.^{19–23} In these complexes the ligand L is $\sigma\text{-N}$, $\mu\text{-N}'$, $\eta^2\text{-CN}'$ (6e) bonded to both Fe atoms (see Figure 1b). Such a coordination mode has also been shown to be present in $[\text{Ru}_2(\text{CO})_4\text{L}_2]$ (L = R-PyCa, R-DAB),^{19–24} $[\text{MnCo}(\text{CO})_6\text{L}]$ (L = R-DAB),²⁵ $[(\mu\text{-H})\text{FeMn}(\text{CO})_6\text{L}]$ (L = R-PyCa),²⁶ $[\text{Ru}_2(\text{CO})_6\text{L}]$ (L = R-DAB),¹⁹ and $[\text{Os}_2(\text{CO})_6\text{L}]$ (L = R-DAB).²⁷

In two instances we succeeded in performing a photochemical change of coordination of an R-DAB ligand. In an argon matrix at 10 K $[\text{Fe}(\text{CO})_3(\sigma\text{-N}, \mu\text{-N}'\text{-R-DAB})]$ was transformed photochemically into $[\text{Fe}(\text{CO})_3(\eta^2, \eta^2\text{-CN}, \text{CN}'\text{-R-DAB})]$ ⁸ and $[(\text{CO})_5\text{MnRe}(\text{CO})_3(\sigma\text{-N}, \mu\text{-N}'\text{-R-DAB})]$ into $[(\text{CO})_3\text{MnRe}(\text{CO})_3(\sigma\text{-N}, \eta^2, \eta^2\text{-CN}, \text{CN}'\text{-R-DAB})]$.¹³ In these two novel complexes the R-DAB ligand is bonded as a 4e- and 8e-donor ligand, respectively. We here present evidence for another change of coordination of an R-PyCa ligand, viz., the transformation of $[\text{Fe}_2(\text{CO})_6(\text{R-PyCa})]$ into $[\text{Fe}_2(\text{CO})_7(\text{R-PyCa})]$ by photolysis under CO in 2-MeTHF. This reaction is accompanied by a change of coordination of the R-PyCa ligand from $\sigma\text{-N}$, $\mu^2\text{-N}'$, $\eta^2\text{-CN}'$ (6e) into $\sigma\text{-N}, \mu\text{-N}'$ (4e).

Experimental Section

Materials and Preparations. The ligands bpy and phen were purchased (Merck) and used without further purification. The preparations of the R-DAB and R-PyCa ligands have been described before.²⁸ The synthesis of $[\text{Fe}_2(\text{CO})_7(\text{L})]$ (L = bpy, phen) has been described by Frühauf.²⁹ The $[\text{Fe}_2(\text{CO})_6(\text{R-DAB})]$ and $[\text{Fe}_2(\text{CO})_6(\text{R-PyCa})]$ complexes were synthesized according to known procedures.²⁰ All phosphines, N-donor ligands, and solvents used were purified by distillation or sublimation and kept under nitrogen. Care was taken to exclude oxygen from the reaction mixtures during the photochemical experiments. The complex $[\text{Fe}_2(\text{CO})_6(\text{bpy})(\text{P}(n\text{-Bu})_3)]$ was prepared by adding 1 mmol of $\text{P}(n\text{-Bu})_3$ to a solution of 1 mmol of $[\text{Fe}_2(\text{CO})_7(\text{bpy})]$ in THF. The solution was stirred at room temperature for approximately 1 h. The color of the solution then changed from red to blue. After evaporation of the solution to dryness, the residue was washed several times with *n*-hexane until the hexane solution became colorless; yield 80%. Single crystals of $[\text{Fe}_2(\text{CO})_6(\text{bpy})(\text{P}(n\text{-Bu})_3)]$ were prepared from a 3:1 mixture of toluene and 2-MeTHF. After the solution was left standing for 1 week at -20°C , suitable crystals had been formed.

(19) Staal, L. H.; Polm, L. H.; Balk, R. W.; van Koten, G.; Vrieze, K.; Brouwers, A. M. F. *Inorg. Chem.* **1980**, *19*, 3343.

(20) Frühauf, H. W.; Landers, A.; Goddard, R.; Krüger, C. *Angew. Chemie*, **1978**, *90*, 56.

(21) Frühauf, H. W.; Breuer, J. J. *Organomet. Chem.* **1984**, *277*, C13.

(22) Frühauf, H. W.; Meijer, D.; Breuer, J. J. *Organomet. Chem.* **1985**, *297*, 221.

(23) Frühauf, H. W.; Breuer, J. J. *Organomet. Chem.* **1986**, *301*, 183.

(24) Polm, L. H.; van Koten, G.; Vrieze, K.; Stam, C. H. *Inorg. Chem.*, in press.

(25) Staal, L. H.; Keijsper, J.; van Koten, G.; Vrieze, K.; Cras, J. A.; Bosman, W. P. *Inorg. Chem.* **1981**, *20*, 555.

(26) Keijsper, J.; Grimberg, P.; van Koten, G.; Vrieze, K.; Kojić-Prodić, B.; Spek, A. L. *Organometallics*, accepted for publication.

(27) Staal, L. H.; van Koten, G.; Vrieze, K. *J. Organomet. Chem.* **1981**, *206*, 99.

(28) Bock, H.; Tom Dieck, H. *Chem. Ber.* **1967**, *100*, 228.

(29) Frühauf, H. W. *J. Chem. Res., Miniprint* **1983**, 2023.

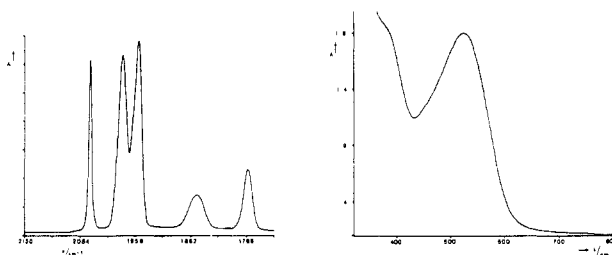


Figure 2. CO-stretching region of the IR spectrum (a) and electronic absorption spectrum (b) of $[\text{Fe}_2(\text{CO})_7(\text{bpy})]$ in 2-MeTHF at 133 and 173 K, respectively.

Crystal data: triclinic; space group $P\bar{1}$; $Z = 2$; cell constants $a = 10.727$ (1) Å, $b = 14.517$ (2) Å, $c = 10.306$ (2) Å, $\alpha = 97.30$ (1)°, $\beta = 96.53$ (1)°, $\gamma = 74.13$ (2)°; $V = 1525.9$ (7) Å³; $F(0,0,0) = 3000$; $d_{\text{calcd}} 1.39$ g cm⁻³; $\mu(\text{Cu K}\alpha) = 85.1$ cm⁻¹; crystal dimensions $0.25 \times 0.35 \times 0.35$ mm. The crystal was sealed in a capillary under nitrogen, and 3815 intensities ($2.5 < \theta < 55^\circ$; $h, -11$ to 11 ; $k, -15$ to 15 ; $l, 0$ to 10) were measured on a Nonius CAD4 diffractometer employing graphite-monochromatized Cu K α radiation. A total of 1390 were below the $3\sigma(I)$ level and were treated as unobserved. The crystal structure was determined by using the heavy-atom method. Refinement proceeded by means of anisotropic block-diagonal least-squares calculations. The H-atom positions were calculated and not refined. An empirical absorption correction (Walker and Stuart, 1983)⁴⁵ was applied. A weighting scheme, $w = (8.4 + F_o + 0.0015F_o^2)^{-1}$ was used, and the anomalous scattering of Fe and P was taken into account. The final R value was 0.057 for the 2425 observed reflections ($R_w = 0.079$). The programs used were from XRAY 76 (Stewart, 1976).⁴⁴ The scattering factors were taken from Cromer and Mann (1968).⁴³

Spectroscopic Measurements. Electronic absorption spectra were recorded on a Perkin-Elmer Lambda 5 UV/vis spectrophotometer and resonance Raman spectra on a Jobin Yvon HG 2S Ramanor using a SP Model 171 argon ion laser as the excitation source. IR spectra were measured on a Nicolet 7199 B FTIR-spectrophotometer with a liquid-nitrogen-cooled Hg, Cd, Te detector (32 scans, resolution = 0.5 cm⁻¹). ³¹P NMR spectra were measured on a Bruker AC 100 spectrometer.

Photochemistry. For the photochemical reactions different lines of a Coherent CR 8 argon ion laser were used as the light source. No reliable quantum yields could be obtained for the reactions of the $[\text{Fe}_2(\text{CO})_7(\text{L})]$ (L = bpy, phen) complexes because of thermal back reactions to the parent compound.

Results and Discussion

I. $[\text{Fe}_2(\text{CO})_7(\text{L})]$ (L = bpy, phen). Spectroscopic Properties. The IR spectrum of $[\text{Fe}_2(\text{CO})_7(\text{bpy})]$ in 2-MeTHF at 133 K (Figure 2) shows a band at 1855 cm⁻¹ belonging to the stretching mode of the semibridging carbonyl and a band at 1763 cm⁻¹ which belongs to the corresponding mode of the nearly symmetrically bridging carbonyl. The absorption spectrum at 173 K in 2-MeTHF shows a broad, intensive band at 528 nm, which is shifted to 524 nm in the spectrum of the corresponding phen complex. This band belongs to one or more MLCT transitions from (a) filled metal d orbital(s) to the lowest π^* level of the α -diimine ligand. This assignment is confirmed by the resonance Raman (rR) spectra of these complexes shown in Figure 3. These spectra were recorded from a solution in a KNO₃ pellet (1.5 mg of complex in 200 mg of KNO₃) at 110 K. They give direct information about the bond changes during an electronic transition since a vibration will only show a strong rR effect when its normal coordinate is severely affected during the electronic transition. The strong rR effects observed in the spectrum of $[\text{Fe}_2(\text{CO})_7(\text{bpy})]$ for the bands at 1025, 1175, 1325, 1492, 1552, and 1605 cm⁻¹, belonging to bpy modes, and for the bands of $[\text{Fe}_2(\text{CO})_7(\text{phen})]$ at 1147, 1210, 1295, 1455, 1510, 1577, and 1630 cm⁻¹, belonging to phen modes, confirm the

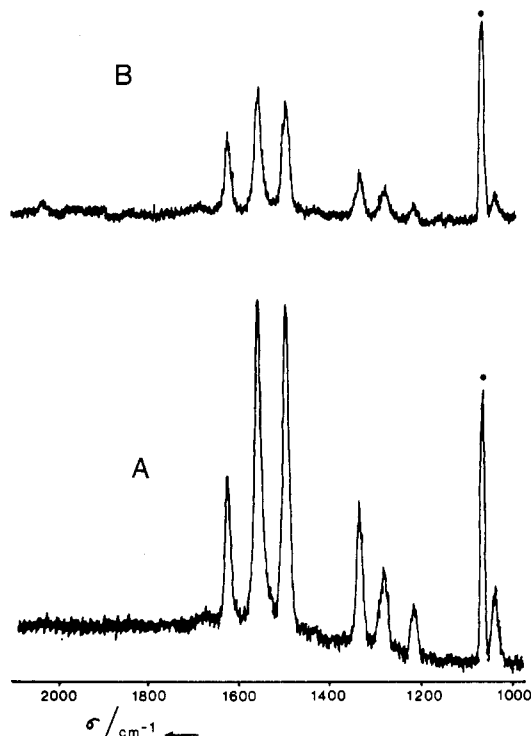


Figure 3. Resonance Raman spectra of $[\text{Fe}_2(\text{CO})_7(\text{bpy})]$ recorded from KNO_3 pellets at 110 K: A, $\lambda_{\text{exc}} = 514.5$ nm; B, $\lambda_{\text{exc}} = 488$ nm. Power was 160 mW (\bullet , KNO_3).

assignment of the absorption band in the visible region to one or more electronic transitions from the metal to the lowest π^* orbital of bpy and phen, respectively.

Apparently, such a transition hardly affects the metal-ligand bonds since only very weak rR effects were observed for the metal-ligand stretching modes. For the corresponding $[\text{M}(\text{CO})_4(\alpha\text{-diimine})]$ ($\text{M} = \text{Cr}, \text{Mo}, \text{W}$)^{6,10} and $[\text{Ph}_3\text{SnMn}(\text{CO})_3(\alpha\text{-diimine})]$ ¹⁶ complexes an extra rR effect was observed for the stretching mode of the carbonyl ligand(s) in the cis position with respect to the α -diimine ligand. This effect has been ascribed to a delocalization of the MLCT state over the cis carbonyl(s). Apparently, no such delocalization is present here, since no rR effect is observed for any carbonyl stretching mode.

Thermal Reactions. The $[\text{Fe}_2(\text{CO})_7(\text{L})]$ complexes readily react thermally with all phosphines used. It appears that these reactions can give two different products. Phosphine ligands with relatively small cone angles³⁰ such as $\text{P}(\text{OMe})_3$ ($\theta = 107^\circ$) or $\text{P}(n\text{-Bu})_3$ ($\theta = 132^\circ$) substitute CO at the metal atom with the α -diimine ligand, giving rise to the formation of $[\text{Fe}_2(\text{CO})_6(\text{bpy})(\text{PR}_3)]$. More bulky phosphines such as PPh_3 ($\theta = 145^\circ$) and $\text{P}(c\text{-Hex})_3$ ($\theta = 170^\circ$) substitute a CO ligand of the less sterically hindered $\text{Fe}(\text{CO})_3$ group. The products then formed are $[\text{Fe}(\text{CO})_3(\text{L})]$ and $[\text{Fe}(\text{CO})_4(\text{PR}_3)]$. For none of these phosphine ligands is found a mixture of products. Moreover, for the dissociative photochemical reaction only one product is formed without any influence of the cone angle of the phosphine on the quantum yield. These observations indicate that the thermal reactions between $[\text{Fe}_2(\text{CO})_7(\text{L})]$ and PR_3 proceed via an associative pathway.

Photochemical Reactions. Figure 4 shows the IR spectral changes in the CO stretching region when $[\text{Fe}_2(\text{CO})_7(\text{bpy})]$ is irradiated ($\lambda_{\text{irr}} = 514.5$ nm, $p = 30$ mW) at 133 K in 2-MeTHF. The reaction shown in Figure 5 takes

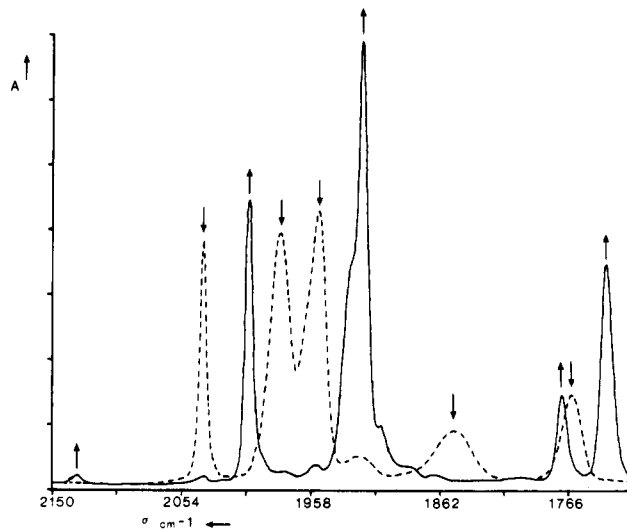


Figure 4. IR spectral changes accompanying the transformation of $[\text{Fe}_2(\text{CO})_7(\text{bpy})]$ into $[\text{Fe}_2(\text{CO})_6(\text{bpy})(\text{S})]$ at 133 K in 2-MeTHF.

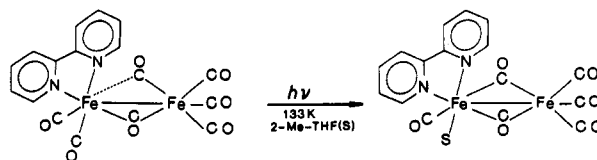


Figure 5. Photochemical reaction of $[\text{Fe}_2(\text{CO})_7(\text{bpy})]$ at 133 K in 2-MeTHF.

place. A CO ligand of the $\text{Fe}(\text{CO})_2(\alpha\text{-diimine})$ moiety is substituted by a solvent molecule, and, contrary to the parent compound, two symmetrically bridging³¹ CO ligands are now present in the photoproduct, which absorb in the IR spectrum at 1771 and 1737 cm^{-1} , respectively. The relative positions of the bands point to a steric equality of these carbonyls; their frequencies show that both bridges are symmetrical.³¹ The conclusion that a CO ligand next to the bpy ligand is photosubstituted can be derived from the close correspondence between the band pattern of this photoproduct and that of $[\text{Fe}_2(\text{CO})_6(\text{bpy})(\text{P}(n\text{-Bu})_3)]$, which has the structure shown in Figure 8. The CO stretching frequencies of the $[\text{Fe}_2(\text{CO})_7(\text{L})]$ complexes and their $[\text{Fe}_2(\text{CO})_6(\text{L})(\text{S})]$ photoproducts are collected in Table I. All carbonyl vibrations of the photoproducts are shifted to lower frequencies with respect to their parent compounds as the result of the photosubstitution. When the temperature of the solution is raised to room temperature, a complete back-reaction to the parent compound takes place. The occurrence of this back-reaction even at low temperatures prevented the determination of reliable quantum yields. Qualitative measurements at 173 K gave an approximate value for these quantum yields of 10^{-2} . In a second experiment the $[\text{Fe}_2(\text{CO})_7(\text{L})]$ complexes were irradiated in 2-MeTHF at 133 K in the presence of excess PR_3 . Care was taken to avoid thermal reactions during the sample preparations. These reactions resulted in the formation of the 2-MeTHF-(S-) substituted complexes $[\text{Fe}_2(\text{CO})_6(\text{L})(\text{S})]$. When the temperature of the solution was raised to 173 K, the solvent molecule was replaced by PR_3 . Similar complexes $[\text{Fe}_2(\text{CO})_6(\text{L})(\text{PR}_3)]$ were directly obtained when the irradiation took place at 173 K. For a comparison of the IR spectrum of the $[\text{Fe}_2(\text{CO})_6(\text{bpy})(\text{P}(\text{OPh})_3)]$ product with that of $[\text{Fe}_2(\text{CO})_6(\text{bpy})(\text{S})]$, both

(30) Tollman, C. A. *Chem. Rev.* 1977, 77, 313.

(31) Crabtree, R. H.; Laven, M. *Inorg. Chem.* 1986, 25, 805.

Table I. IR and UV/Vis Spectral Data of Several Binuclear $[\text{Fe}_2(\text{CO})_x(\alpha\text{-diimine})]$ ($x = 6, 7$) Complexes and Their Photosubstitution Products

complex	CO stretching freq. cm^{-1}	λ , nm
1. $[\text{Fe}_2(\text{CO})_6(p\text{-Tol-PyCa})]$	2057 (s), 1996 (vs), 1980 (s), 1971 (s), 1927 (s)	515 (sh)
2. $[\text{Fe}_2(\text{CO})_6(c\text{-Hex-PyCa})]$	2054 (s), 1995 (vs), 1980 (s), 1971 (s), 1927 (s)	520 (sh)
3. $[\text{Fe}_2(\text{CO})_6(i\text{-Pr-DAB})]$	2053 (s), 1995 (vs), 1976 (s), 1968 (s), 1926 (s)	530 (sh)
photoproduct ^a	2013 (m), 1971 (s), 1942 (m), 1915 (m), 1830 (w)	480
4. $[\text{Fe}_2(\text{CO})_6(p\text{-Tol-DAB})]$	2061 (s), 2003 (vs), 1984 (s), 1938 (s), 1930 (s)	540 (sh)
photoproduct ^a	2024 (m), 1985 (s), 1956 (m), 1934 (m), 1825 (w)	498
5. $[\text{Fe}_2(\text{CO})_6(c\text{-Hex-DAB})]$	2053 (s), 1990 (vs), 1976 (s), 1967 (s), 1923 (s)	535 (sh)
photoproduct ^a	2012 (m), 1969 (s), 1940 (m), 1914 (m), 1828 (w)	474
6. $[\text{Fe}_2(\text{CO})_6(t\text{-Bu-DAB})]$	2051 (s), 1993 (vs), 1963 (s), 1926 (s)	530 (sh)
photoproduct ^a	2009 (m), 1962 (s), 1937 (m), 1907 (m), 1829 (w)	482
7. $[\text{Fe}_2(\text{CO})_7(\text{bpy})]$	2038 (s), 1980 (s), 1952 (s), 1855 (w), 1763 (w)	528
8. $[\text{Fe}_2(\text{CO})_7(\text{phen})]$	2039 (s), 1981 (s), 1963 (s), 1851 (w), 1773 (w)	524
9. $[\text{Fe}_2(\text{CO})_7(p\text{-Tol-PyCa})]$	2043 (s), 1984 (s), 1963 (s), 1869 (w), 1773 (w)	574
10. $[\text{Fe}_2(\text{CO})_7(c\text{-Hex-PyCa})]$	2039 (s), 1980 (s), 1957 (s), 1860 (s), 1769 (w)	533
11. $[\text{Fe}_2(\text{CO})_6(\text{bpy})(\text{S})]$	2005 (s), 1919 (vs), 1771 (w), 1737 (m)	br
12. $[\text{Fe}_2(\text{CO})_6(\text{phen})(\text{S})]$	2004 (s), 1920 (vs), 1771 (w), 1738 (m)	br
13. $[\text{Fe}_2(\text{CO})_6(p\text{-Tol-PyCa})(\text{S})]$	2011 (s), 1927 (vs), 1771 (w), 1739 (m)	605
14. $[\text{Fe}_2(\text{CO})_6(c\text{-Hex-PyCa})(\text{S})]$	2007 (s), 1925 (vs), 1771 (w), 1738 (m)	600
15. $[\text{Fe}_2(\text{CO})_6(\text{bpy})(\text{P}(n\text{-Bu})_3)]$	2002 (s), 1926 (sh), 1921 (s), 1805 (w), 1735 (w)	b
16. $[\text{Fe}_2(\text{CO})_6(\text{bpy})(\text{P}(c\text{-Hex})_3)]$	1999 (s), 1917 (s), 1768 (w), 1737 (m)	b
17. $[\text{Fe}_2(\text{CO})_6(\text{bpy})(\text{P}(\text{Ph})_3)]$	2004 (s), 1927 (s), 1809 (w), 1741 (m)	b
18. $[\text{Fe}_2(\text{CO})_6(\text{bpy})(\text{P}(\text{OMe})_3)]$	2006 (s), 1927 (sh), 1923 (s), 1812 (w), 1748 (m)	b
19. $[\text{Fe}_2(\text{CO})_6(\text{bpy})(\text{P}(\text{OPh})_3)]$	2014 (s), 1944 (sh), 1933 (s), 1832 (w), 1753 (w)	b
20. $[\text{Fe}_2(\text{CO})_6(\text{bpy})(\text{py})]$	2001 (s), 1917 (s), 1775 (w), 1733 (m)	b
21. $[\text{Fe}_2(\text{CO})_6(\text{bpy})(n\text{-propylamine})]$	1995 (s), 1913 (s), 1767 (w), 1727 (m)	b
22. $[\text{Fe}_2(\text{CO})_6(\text{bpy})(\text{CH}_3\text{CN})]$	2004 (s), 1919 (vs), 1777 (m), 1744 (m)	b
23. $[\text{Fe}_2(\text{CO})_6(\text{phen})(\text{P}(n\text{-Bu})_3)]$	2001 (s), 1922 (s), 1803 (w), 1734 (w)	b
24. $[\text{Fe}_2(\text{CO})_6(\text{phen})(\text{P}(\text{Ph})_3)]$	2004 (s), 1926 (s), 1807 (w), 1740 (m)	b
25. $[\text{Fe}_2(\text{CO})_6(\text{phen})(\text{P}(\text{OPh})_3)]$	2015 (s), 1935 (s), 1830 (w), 1751 (m)	b

^aIn 2-MeTHF at 133 K. ^bExact positions were not measured; all these products are blue in 2-MeTHF solution at 133 K. Spectra 3–6 and 11–25 were taken from 133 K 2-MeTHF solutions. Spectra 1, 2, and 7–10 were taken from 173 K 2-MeTHF solutions. Abbreviations: vs, very strong; s, strong; m, medium; w, weak; sh, shoulder.

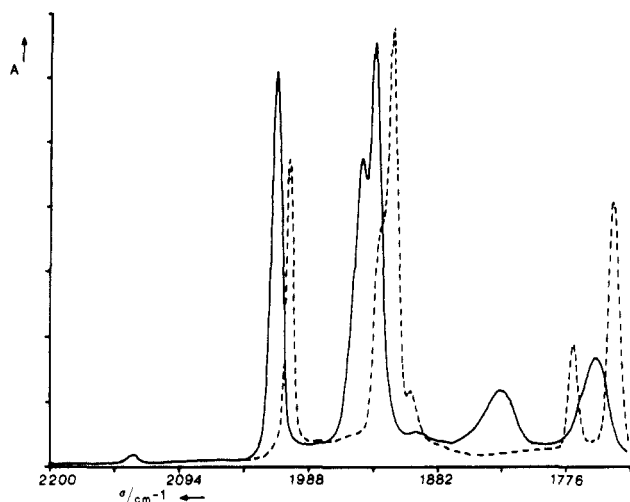


Figure 6. IR spectra of $[\text{Fe}_2(\text{CO})_6(\text{bpy})(\text{S})]$ (dashed) and $[\text{Fe}_2(\text{CO})_6(\text{bpy})(\text{P}(\text{OPh})_3)]$ (drawn) in the CO stretching region at 133 K in 2-MeTHF.

spectra were recorded at 133 K (see Figure 6). The CO frequencies of all PR_3 -substituted products are also collected in Table I. There appears to be a gradual decrease of the carbonyl frequencies when the substituting ligand becomes more basic. One of the bands in particular shows a dramatic shift to lower frequency. For the series of complexes $[\text{Fe}_2(\text{CO})_6(\text{bpy})(\text{L})]$ ($\text{L} = \text{CO}, \text{P}(\text{OPh})_3, \text{PPh}_3, \text{S}$) this band is found at 1855, 1832, 1809, and 1771 cm^{-1} , respectively. It is assigned to the stretching mode of the carbonyl ligand trans to the substituent, which is symmetrically bridging in the 2-MeTHF product but semi-bridging in the PR_3 complexes. This conclusion is confirmed by the crystal structure of the $\text{P}(n\text{-Bu})_3$ product (vide infra). The only exception here is the $\text{P}(c\text{-Hex})_3$

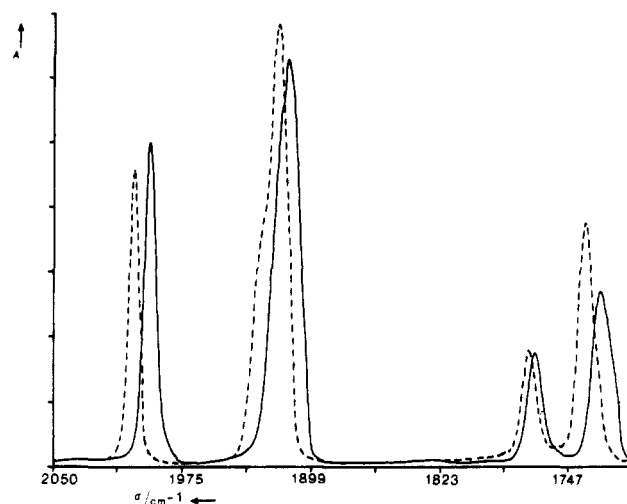


Figure 7. IR spectra of $[\text{Fe}_2(\text{CO})_6(\text{bpy})(\text{S})]$ (dashed) and $[\text{Fe}_2(\text{CO})_6(\text{bpy})(n\text{-propylamine})]$ (drawn) in the CO stretching region at 133 K in 2-MeTHF.

product, in which still two symmetrically bridging carbonyls are present. This exceptional behavior of $\text{P}(c\text{-Hex})_3$ is most probably due to its bulkiness. Because of that the Fe–P distance will be larger in this complex than, e.g., in the photoproduct of $\text{P}(n\text{-Bu})_3$, which ligand has similar electronic properties. Apparently, this lengthening of the Fe–P bond primarily causes a decrease of π -back-bonding to the phosphine ligand with a concomitant increase of π -back-bonding to the trans-bridging carbonyl. When the solutions of the photoproducts are warmed up to room temperature, the $\text{P}(n\text{-Bu})_3$ product appears to be the most stable one. However, also this complex shows a slow back-reaction to the parent compound with free CO from the solution. Low-temperature photochemical reactions

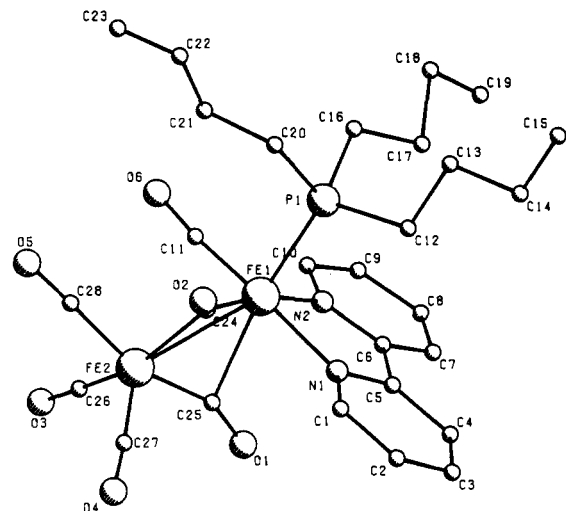


Figure 8. Crystal structure (PLUTO drawing) of $[\text{Fe}_2(\text{CO})_6(\text{bpy})(\text{P}(n\text{-Bu})_3)]$.

were also performed in the presence of N-donor ligands. The ligands used are CH_3CN , pyridine, and *n*-propylamine. Irradiation at 133 K of $[\text{Fe}_2(\text{CO})_7(\text{bpy})]$ in the presence of these N-donor ligands again resulted in the formation of the 2-MeTHF-substituted complex. At 173 K the solvent molecule was replaced by the N-donor ligand. Table I shows the carbonyl frequencies of these complexes, $[\text{Fe}_2(\text{CO})_6(\text{bpy})(\text{L}')] (L' = \text{CH}_3\text{CN}, \text{pyridine}, n\text{-propylamine})$, and Figure 7 compares the IR spectra of $[\text{Fe}_2(\text{CO})_6(\text{bpy})(\text{S})]$ and $[\text{Fe}_2(\text{CO})_6(\text{bpy})(n\text{-propylamine})]$ at 133 K. Raising the temperature of the solution again resulted in a back-reaction with CO to the parent compound. Just as in the 2-MeTHF-substituted complex, but contrary to the parent compound and the phosphine-substituted ones, both bridging carbonyls are symmetrically bridging in these N-donor complexes. This is due to the trans influence of the substituting ligand on one of these bridges. The phosphine ligands are soft bases that can accept negative charge from the metal atom by π -back-donation. In the complexes of the N-donor ligands and 2-MeTHF, which are all hard bases, the metal compensates for the extra charge donated by these ligands, by an increase of π -back-bonding to the bridging carbonyl in the trans position.

Crystal Structure of $[\text{Fe}_2(\text{CO})_6(\text{bpy})(\text{P}(n\text{-Bu})_3)]$. A crystal structure determination of this photoproduct yielded the molecular structure, shown in Figure 8. The final coordinates of the atoms are listed in Table II and selected bond lengths and bond angles in Table III. In Table IV the anisotropic thermal parameters of the non-hydrogen atoms are listed. A comparison of this structure with that of $[\text{Fe}_2(\text{CO})_7(\text{bpy})]$, determined by Cotton,¹⁸ shows that the metal-metal distances in both complexes are nearly equal (2.6048 and 2.611 Å, respectively). So, substitution of a CO ligand by $\text{P}(n\text{-Bu})_3$ has no effect on this bond length. The Fe1 atom is nearly octahedrally surrounded. The equatorial plane consists of the Fe1-N1 bond, the Fe1-N2 bond, the Fe1-C24 bond, and the Fe1-C11 bond. The axial positions are occupied by the phosphine ligand and the carbon atom C25 (the relevant bond angles are marked in Table III). The Fe1-N bond lengths are 2.016 and 1.998 Å, respectively. They are larger than the Fe-N bond lengths in the $[\text{Fe}(\text{CO})_3(2,6\text{-}i\text{-Pr}_2\text{Ph-DAB})]$ ⁷ and $[\text{Fe}(\text{CO})_3(\text{tetraazadiene})]$ complexes³² due to

Table II. Fractional Coordinates and Equivalent Isotropic Thermal Parameters with Estimated Standard Deviations in Parentheses

atom	x	y	z	$U_{\text{eq}}, \text{\AA}^2$
Fe(1)	0.79020 (12)	0.27348 (9)	0.09558 (12)	0.0390 (7)
Fe(2)	0.70837 (13)	0.20225 (11)	-0.13276 (13)	0.0545 (9)
P(1)	0.80862 (23)	0.25331 (16)	0.31329 (21)	0.0440 (13)
C(1)	1.0690 (8)	0.1580 (6)	0.0649 (8)	0.047 (5)
C(2)	1.2004 (8)	0.1461 (7)	0.0632 (9)	0.056 (6)
C(3)	1.2514 (9)	0.2244 (7)	0.0870 (9)	0.061 (6)
C(4)	1.1684 (8)	0.3134 (6)	0.1120 (8)	0.050 (5)
C(5)	1.0347 (7)	0.3227 (6)	0.1118 (7)	0.039 (5)
C(6)	0.9358 (8)	0.4150 (6)	0.1313 (8)	0.045 (5)
C(7)	0.9683 (9)	0.5016 (6)	0.1567 (8)	0.054 (6)
C(8)	0.8702 (11)	0.5861 (7)	0.1720 (10)	0.073 (7)
C(9)	0.7444 (11)	0.5806 (7)	0.1608 (11)	0.075 (7)
C(10)	0.7166 (10)	0.4900 (7)	0.1337 (10)	0.066 (6)
C(11)	0.6201 (9)	0.3120 (7)	0.0928 (9)	0.058 (6)
C(12)	0.9768 (9)	0.2138 (7)	0.3845 (8)	0.059 (6)
C(13)	0.9987 (11)	0.1899 (8)	0.5288 (9)	0.074 (7)
C(14)	1.1396 (11)	0.1673 (9)	0.5791 (11)	0.087 (8)
C(15)	1.1585 (12)	0.1424 (9)	0.7176 (11)	0.090 (8)
C(16)	0.7334 (10)	0.3599 (8)	0.4221 (10)	0.071 (7)
C(17)	0.8079 (12)	0.4315 (7)	0.4601 (11)	0.077 (7)
C(18)	0.7103 (20)	0.5227 (11)	0.5524 (25)	0.208 (20)
C(19)	0.7649 (23)	0.5835 (21)	0.5482 (15)	0.254 (22)
C(20)	0.7389 (11)	0.1620 (8)	0.3602 (10)	0.077 (8)
C(21)	0.5989 (13)	0.1713 (10)	0.3238 (13)	0.099 (10)
C(22)	0.5477 (16)	0.1038 (14)	0.3843 (19)	0.159 (16)
C(23)	0.4452 (26)	0.0860 (17)	0.3611 (25)	0.220 (25)
C(24)	0.7915 (8)	0.1462 (6)	0.0483 (8)	0.048 (5)
C(25)	0.8043 (8)	0.2883 (7)	-0.1160 (8)	0.055 (6)
C(26)	0.6042 (10)	0.2737 (9)	-0.2482 (10)	0.081 (8)
C(27)	0.8101 (10)	0.1050 (7)	-0.2247 (10)	0.067 (7)
C(28)	0.5828 (10)	0.1500 (8)	-0.1039 (10)	0.076 (7)
N(1)	0.9838 (6)	0.2443 (4)	0.0890 (6)	0.038 (4)
N(2)	0.8131 (6)	0.4070 (5)	0.1230 (6)	0.043 (4)
O(1)	0.8600 (7)	0.3392 (5)	-0.1533 (6)	0.073 (5)
O(2)	0.8205 (7)	0.0668 (4)	0.0786 (6)	0.067 (4)
O(3)	0.5377 (9)	0.3183 (9)	-0.3263 (9)	0.144 (9)
O(4)	0.8721 (9)	0.0414 (6)	-0.2876 (8)	0.101 (6)
O(5)	0.5049 (8)	0.1125 (7)	-0.0879 (9)	0.117 (7)
O(6)	0.5090 (6)	0.3429 (5)	0.1007 (7)	0.078 (5)
H(1)	1.033 (0)	0.093 (0)	0.048 (0)	0.06 (0)
H(2)	1.265 (0)	0.073 (0)	0.045 (0)	0.06 (0)
H(3)	1.356 (0)	0.215 (0)	0.085 (0)	0.06 (0)
H(4)	1.205 (0)	0.378 (0)	0.133 (0)	0.06 (0)
H(7)	1.071 (0)	0.502 (0)	0.163 (0)	0.06 (0)
H(8)	0.893 (0)	0.656 (0)	0.194 (0)	0.06 (0)
H(9)	0.665 (0)	0.647 (0)	0.172 (0)	0.06 (0)
H(10)	0.613 (0)	0.488 (0)	0.126 (0)	0.06 (0)
H(121)	1.027 (0)	0.152 (0)	0.324 (0)	0.06 (0)
H(122)	1.023 (0)	0.273 (0)	0.378 (0)	0.06 (0)
H(131)	0.945 (0)	0.252 (0)	0.594 (0)	0.06 (0)
H(132)	0.960 (0)	0.130 (0)	0.539 (0)	0.06 (0)
H(141)	1.192 (0)	0.107 (0)	0.517 (0)	0.06 (0)
H(142)	1.176 (0)	0.229 (0)	0.575 (0)	0.06 (0)
H(151)	1.106 (0)	0.202 (0)	0.779 (0)	0.06 (0)
H(152)	1.121 (0)	0.080 (0)	0.722 (0)	0.06 (0)
H(153)	1.260 (0)	0.125 (0)	0.751 (0)	0.06 (0)
H(161)	0.641 (0)	0.396 (0)	0.373 (0)	0.06 (0)
H(162)	0.715 (0)	0.336 (0)	0.511 (0)	0.06 (0)
H(171)	0.897 (0)	0.402 (0)	0.517 (0)	0.06 (0)
H(172)	0.829 (0)	0.460 (0)	0.375 (0)	0.06 (0)
H(181)	0.611 (0)	0.539 (0)	0.503 (0)	0.06 (0)
H(182)	0.704 (0)	0.499 (0)	0.647 (0)	0.06 (0)
H(191)	0.863 (0)	0.569 (0)	0.603 (0)	0.06 (0)
H(192)	0.770 (0)	0.608 (0)	0.459 (0)	0.06 (0)
H(193)	0.702 (0)	0.644 (0)	0.614 (0)	0.06 (0)
H(201)	0.791 (0)	0.093 (0)	0.316 (0)	0.06 (0)
H(202)	0.753 (0)	0.163 (0)	0.466 (0)	0.06 (0)
H(211)	0.545 (0)	0.244 (0)	0.352 (0)	0.06 (0)
H(212)	0.585 (0)	0.155 (0)	0.219 (0)	0.06 (0)
H(221)	0.622 (0)	0.035 (0)	0.378 (0)	0.06 (0)
H(222)	0.551 (0)	0.131 (0)	0.492 (0)	0.06 (0)
H(231)	0.373 (0)	0.155 (0)	0.372 (0)	0.06 (0)
H(232)	0.444 (0)	0.059 (0)	0.258 (0)	0.06 (0)
H(233)	0.408 (0)	0.037 (0)	0.408 (0)	0.06 (0)

(32) Doedens, R. J. *J. Chem. Soc., Chem. Commun.* 1968, 1271.

Table III. Bond Lengths (Å) and Selected Bond Angles (deg) with Esd's in Parentheses

Bond Angles			
Fe(2)-Fe(1)-P(1)	141.60 (7)	C(24)-Fe(2)-C(25)	93.2 (4)
Fe(2)-Fe(1)-C(11)	75.5 (3)	C(24)-Fe(2)-C(26)	161.5 (3)
Fe(2)-Fe(1)-C(24)	54.1 (2)	C(24)-Fe(2)-C(27)	92.0 (4)
Fe(2)-Fe(1)-C(25)	42.9 (2)	C(24)-Fe(2)-C(28)	81.7 (4)
Fe(2)-Fe(1)-N(1)	104.4 (2)	C(25)-Fe(2)-C(26)	86.8 (5)
Fe(2)-Fe(1)-N(2)	121.3 (2)	C(25)-Fe(2)-C(27)	100.1 (5)
P(1)-Fe(1)-C(11)	91.5 (0) ^a	C(25)-Fe(2)-C(28)	158.4 (4)
P(1)-Fe(1)-C(24)	91.8 (3) ^a	C(26)-Fe(2)-C(27)	106.3 (5)
P(1)-Fe(1)-C(25)	171.5 (2) ^a	C(26)-Fe(2)-C(28)	91.5 (6)
P(1)-Fe(1)-N(1)	92.7 (2) ^a	C(27)-Fe(2)-C(28)	101.1 (5)
P(1)-Fe(1)-N(2)	95.2 (2) ^a	Fe(1)-P(1)-C(12)	114.1 (3)
C(11)-Fe(1)-C(24)	93.4 (4) ^a	Fe(1)-P(1)-C(16)	115.9 (3)
C(11)-Fe(1)-C(25)	96.9 (4) ^a	Fe(1)-P(1)-C(20)	117.0 (3)
C(11)-Fe(1)-N(1)	173.0 (4) ^a	Fe(1)-C(11)-O(6)	174.0 (5)
C(11)-Fe(1)-N(2)	94.2 (4) ^a	Fe(1)-C(24)-Fe(2)	81.4 (4)
C(24)-Fe(1)-C(25)	88.6 (4) ^a	Fe(1)-C(24)-O(2)	147.5 (5)
C(24)-Fe(1)-N(1)	92.1 (4) ^a	Fe(2)-C(24)-O(2)	131.0 (5)
C(24)-Fe(1)-N(2)	169.5 (3) ^a	Fe(1)-C(25)-Fe(2)	79.2 (4)
C(25)-Fe(1)-N(1)	78.8 (3) ^a	Fe(1)-C(25)-O(1)	124.8 (5)
C(25)-Fe(1)-N(2)	83.4 (3) ^a	Fe(2)-C(25)-O(1)	156.0 (5)
N(1)-Fe(1)-N(2)	79.8 (3) ^a	Fe(2)-C(26)-O(3)	178.0 (6)
Fe(1)-Fe(2)-C(24)	44.5 (2)	Fe(2)-C(27)-O(4)	177.4 (5)
Fe(1)-Fe(2)-C(25)	57.8 (2)	Fe(2)-C(28)-O(5)	177.0 (6)
Fe(1)-Fe(2)-C(26)	123.1 (3)	Fe(1)-N(1)-C(1)	128.1 (4)
Fe(1)-Fe(2)-C(27)	121.5 (3)	Fe(1)-N(1)-C(5)	115.5 (5)
Fe(1)-Fe(2)-C(28)	106.4 (3)		
Bond Lengths			
Fe(1)-Fe(2)	2.6048 (14)	C(6)-C(7)	1.380 (9)
Fe(1)-P(1)	2.279 (2)	C(6)-N(2)	1.345 (8)
Fe(1)-C(11)	1.754 (7)	C(7)-C(8)	1.385 (10)
Fe(1)-C(24)	1.847 (6)	C(8)-C(9)	1.364 (13)
Fe(1)-C(25)	2.244 (6)	C(9)-C(10)	1.414 (10)
Fe(1)-N(1)	2.010 (5)	C(10)-N(2)	1.359 (9)
Fe(1)-N(2)	2.001 (5)	C(11)-O(6)	1.162 (9)
Fe(2)-C(24)	2.133 (6)	C(12)-C(13)	1.547 (9)
Fe(2)-C(25)	1.805 (7)	C(13)-C(14)	1.501 (12)
Fe(2)-C(26)	1.766 (8)	C(14)-C(15)	1.495 (12)
Fe(2)-C(27)	1.770 (7)	C(16)-C(17)	1.467 (11)
Fe(2)-C(28)	1.785 (8)	C(17)-C(18)	1.70 (2)
P(1)-C(12)	1.834 (7)	C(18)-C(19)	1.19 (2)
P(1)-C(16)	1.840 (8)	C(20)-C(21)	1.480 (13)
P(1)-C(20)	1.826 (9)	C(21)-C(22)	1.48 (2)
C(1)-C(2)	1.375 (9)	C(22)-C(23)	1.19 (2)
C(1)-N(1)	1.347 (8)	C(24)-O(2)	1.182 (7)
C(2)-C(3)	1.375 (10)	C(25)-O(1)	1.189 (9)
C(3)-C(4)	1.367 (10)	C(26)-O(3)	1.151 (11)
C(4)-C(5)	1.403 (9)	C(27)-O(4)	1.151 (9)
C(5)-C(6)	1.471 (8)	C(28)-O(5)	1.151 (10)
C(5)-N(1)	1.376 (7)		

^a Relevant bond angles.

the poor π -accepting ability of the bpy ligand compared to the other two ligands.

The most interesting features of the structure are the bridging carbonyls. Figure 9 schematically shows the $\text{Fe}_2(\text{CO})_2$ units of the $\text{P}(n\text{-Bu})_3$ -substituted complex and of $[\text{Fe}_2(\text{CO})_7(\text{bpy})]$, together with the bond lengths and bond angles. From the shortening of the Fe1-C25 and Fe1-C24 bonds and the lengthening of the Fe2-C25 and Fe2-C24 ones, it can be concluded that the bridging carbonyls move toward the Fe1 atom when this metal center becomes more basic by the substitution of CO by $\text{P}(n\text{-Bu})_3$. This effect, which is most pronounced for the bridging carbonyl trans to the coordinated phosphine, represents a clear trans influence of the phosphine on the bridging behavior. Note also the decrease in the Fe1-Fe2-C25 angle going from $[\text{Fe}_2(\text{CO})_7(\text{bpy})]$ to $[\text{Fe}_2(\text{CO})_6(\text{bpy})\text{P}(n\text{-Bu})_3]$. Recently, Crabtree and Lavin presented a structural analysis of the semibridging carbonyl.³¹ In view of their results we can conclude from the crystal structures of the

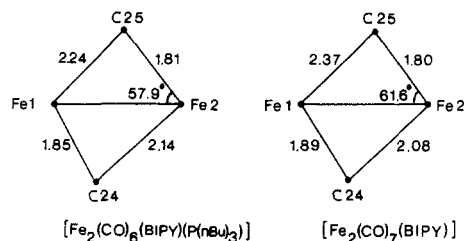


Figure 9. Schematic representation of the bridging behavior with relevant bond lengths and angles in $[\text{Fe}_2(\text{CO})_7(\text{bpy})]$ and $[\text{Fe}_2(\text{CO})_6(\text{bpy})\text{P}(n\text{-Bu})_3]$.

parent compound and of the $\text{P}(n\text{-Bu})_3$ -substituted product that in both complexes one of the carbonyls is nearly symmetrically bridging. The other carbonyl (trans in the photoproduct with respect to $\text{P}(n\text{-Bu})_3$) is bent symmetrically bridging (bsb) in both complexes but more bent toward Fe1 in $[\text{Fe}_2(\text{CO})_6(\text{bpy})\text{P}(n\text{-Bu})_3]$. This effect on the bridges is clearly in line with the proposal that bridging plays an important role in clusters for the delocalization of excess negative charge.^{33,34}

The ³¹P NMR spectrum of the complex in THF shows one singlet at 28 ppm (free $\text{P}(n\text{-Bu})_3$, -32 ppm). The rR spectrum as well as some interesting reactions of this complex will be described in a forthcoming paper.

The Photochemical Mechanism. The question remains from which excited state the photochemical reaction takes place. Irradiation takes place into the MLCT transitions from the metal d orbitals to the lowest π^* level of the α -diimine ligand. Normally, such MLCT states are not reactive, since the loss of π -back-bonding is often compensated by the increase of ionic interaction. Reactions can, however, take place from a close-lying reactive state as, e.g., in the case of $\text{Ru}(\text{bpy})_3^{2+}$.³⁵ This latter complex is relatively photostable at room temperature but photodecomposes upon raising the temperature because of thermal occupation of a reactive LF state. Similar close-lying MLCT and LF states have been shown to be present in the complexes $[\text{Ru}(\text{NH}_3)_5(\text{py-X})^{2+}]$ ^{36,37} and $[\text{M}(\text{CO})_5(\text{L})]$ (M = Cr, Mo, W; L = py-X, pyridazine).^{38,39} Because of these reactive LF states, the photosubstitution quantum yields of these complexes can be rather high, from 10^{-2} to values of $\Phi > 0.1$. Quantitative quantum yields could not be determined for the complexes $[\text{Fe}_2(\text{C}-\text{O})_7(\text{L})]$ because of the thermal back-reactions to the parent compound. However, when these back-reactions were not taken into account, minimal values of about 10^{-2} were obtained. This points to a reaction from a reactive LF state close in energy to the MLCT state, since the latter state is normally not reactive. Support for this assumption is provided by the results obtained for the mononuclear analogues $[\text{Fe}(\text{CO})_3(\text{R-DAB})]$.⁴⁰ MO calculations on the binuclear complex $[\text{Fe}_2(\text{CO})_5(\text{PH}_3)_4]$ have shown that this compound does not possess a metal-metal bond but is instead composed of two $\text{Fe}(\text{CO})_2(\text{PH}_3)_2$ fragments linked

(33) Cotton, F. A. *Prog. Inorg. Chem.* 1976, 21, 1.(34) Horwitz, C. P.; Shriver, D. F. *Adv. Organomet. Chem.* 1984, 23, 219.(35) Durham, B.; Caspar, J. V.; Nagle, J. K.; Meijer, T. J. *J. Am. Chem. Soc.* 1982, 104, 4803.(36) Malouf, G.; Ford, P. C. *J. Am. Chem. Soc.* 1974, 96, 601.(37) Malouf, G.; Ford, P. C. *J. Am. Chem. Soc.* 1977, 99, 7213.(38) Balk, R. W.; Boxhoorn, G.; Snoeck, T. L.; Schoemaker, G. C.; Stufkens, D. J.; Oskam, A. *J. Chem. Soc., Dalton Trans.* 1981, 1524.(39) Adamson, A. W. *Comments Inorg. Chem.* 1981, 1, 33.

(40) van Dijk, H. K.; Stufkens, D. J.; Oskam, A., to be submitted for publication.

Table IV. Anisotropic Thermal Parameters

atom	U(11)	U(22)	U(33)	U(12)	U(13)	U(23)
Fe(1)	0.0394 (7)	0.0364 (7)	0.0414 (7)	-0.0107 (6)	0.0024 (6)	0.0039 (6)
Fe(2)	0.0455 (8)	0.0720 (10)	0.0451 (8)	-0.0187 (7)	0.0016 (6)	-0.0035 (7)
P(1)	0.0523 (14)	0.0433 (13)	0.0379 (12)	-0.0115 (11)	0.0081 (10)	0.0076 (10)
C(1)	0.039 (5)	0.049 (5)	0.050 (5)	-0.004 (4)	0.004 (4)	0.007 (4)
C(2)	0.045 (5)	0.062 (6)	0.054 (5)	-0.004 (5)	-0.001 (4)	0.006 (5)
C(3)	0.044 (5)	0.077 (7)	0.064 (6)	-0.021 (5)	0.005 (4)	0.001 (5)
C(4)	0.050 (5)	0.061 (6)	0.047 (5)	-0.026 (5)	0.007 (4)	0.005 (4)
C(5)	0.039 (5)	0.044 (5)	0.033 (4)	-0.006 (4)	0.001 (3)	0.011 (4)
C(6)	0.059 (6)	0.041 (5)	0.039 (5)	-0.018 (4)	0.002 (4)	0.011 (4)
C(7)	0.075 (7)	0.049 (5)	0.044 (5)	-0.027 (5)	0.012 (5)	0.002 (4)
C(8)	0.113 (9)	0.043 (6)	0.069 (7)	-0.027 (6)	0.020 (6)	0.001 (5)
C(9)	0.098 (8)	0.045 (6)	0.081 (7)	-0.004 (6)	0.028 (6)	0.015 (5)
C(10)	0.070 (7)	0.050 (6)	0.068 (6)	0.003 (5)	0.006 (5)	0.016 (5)
C(11)	0.056 (6)	0.051 (6)	0.068 (6)	-0.011 (5)	0.004 (5)	0.011 (5)
C(12)	0.067 (6)	0.065 (6)	0.036 (5)	0.004 (5)	0.005 (4)	0.012 (4)
C(13)	0.084 (8)	0.086 (8)	0.046 (6)	-0.010 (6)	0.000 (5)	0.025 (5)
C(14)	0.078 (8)	0.105 (9)	0.069 (7)	-0.004 (7)	0.001 (6)	0.021 (7)
C(15)	0.102 (9)	0.085 (8)	0.067 (7)	-0.002 (7)	-0.019 (6)	0.022 (6)
C(16)	0.069 (7)	0.076 (7)	0.065 (6)	-0.011 (6)	0.018 (5)	0.001 (6)
C(17)	0.104 (9)	0.048 (6)	0.074 (7)	-0.009 (6)	0.018 (6)	0.001 (5)
C(18)	0.203 (20)	0.065 (10)	0.335 (20)	-0.052 (11)	-0.124 (20)	0.019 (14)
C(19)	0.231 (23)	0.379 (34)	0.060 (10)	0.112 (23)	0.025 (12)	0.083 (15)
C(20)	0.094 (8)	0.074 (7)	0.073 (7)	-0.027 (6)	0.015 (6)	0.025 (6)
C(21)	0.106 (10)	0.113 (10)	0.104 (9)	-0.054 (8)	0.028 (8)	0.025 (8)
C(22)	0.143 (14)	0.198 (18)	0.199 (18)	-0.135 (14)	0.049 (13)	0.025 (14)
C(23)	0.282 (28)	0.200 (22)	0.239 (25)	-0.127 (20)	-0.004 (21)	0.134 (20)
C(24)	0.049 (5)	0.044 (5)	0.054 (5)	-0.025 (4)	0.005 (4)	-0.008 (4)
C(25)	0.042 (5)	0.078 (7)	0.040 (5)	-0.010 (5)	-0.005 (4)	0.009 (5)
C(26)	0.065 (7)	0.126 (10)	0.054 (6)	-0.031 (7)	-0.010 (5)	0.014 (6)
C(27)	0.075 (7)	0.064 (7)	0.064 (6)	-0.016 (6)	0.010 (5)	0.009 (5)
C(28)	0.058 (7)	0.102 (9)	0.070 (7)	-0.035 (6)	0.007 (5)	-0.010 (6)
N(1)	0.036 (4)	0.038 (4)	0.039 (4)	-0.012 (3)	-0.001 (3)	0.004 (3)
N(2)	0.048 (4)	0.038 (4)	0.041 (4)	-0.009 (3)	0.004 (3)	0.007 (3)
O(1)	0.095 (5)	0.083 (5)	0.054 (4)	-0.036 (4)	0.008 (4)	0.020 (4)
O(2)	0.084 (5)	0.045 (4)	0.075 (4)	-0.026 (3)	0.006 (4)	0.000 (3)
O(3)	0.092 (7)	0.223 (12)	0.104 (7)	-0.004 (7)	-0.024 (5)	0.078 (8)
O(4)	0.131 (7)	0.072 (5)	0.098 (6)	-0.017 (5)	0.011 (5)	-0.012 (4)
O(5)	0.087 (6)	0.155 (9)	0.125 (7)	-0.066 (6)	0.026 (5)	-0.016 (6)
O(6)	0.051 (4)	0.082 (5)	0.095 (5)	-0.005 (4)	0.014 (4)	0.008 (4)

by a bridging carbonyl.⁴¹ Similarly, the $[\text{Fe}_2(\text{CO})_7(\text{L})]$ complexes are considered to consist of two fragments, $\text{Fe}(\text{CO})_2(\text{L})$ and $\text{Fe}(\text{CO})_4$, respectively, which are linked by a bridging carbonyl ligand. The electronic structure of the $\text{Fe}(\text{CO})_2(\text{L})$ fragment will therefore be comparable to that of the $[\text{Fe}(\text{CO})_3(\text{R-DAB})]$ complex, and this correspondence is, e.g., reflected in a similar position of the MLCT band in both complexes. Now, irradiation of $[\text{Fe}(\text{CO})_3(\text{R-DAB})]$ into the MLCT band ($\lambda_{\text{max}} \approx 500 \text{ nm}$) in the presence of a phosphine ligand causes the photo-substitution of a CO ligand. The quantum yield of this reaction increases upon going to higher energy excitation which points to a reaction from a close-lying reactive LF state. Since, however, no LF transition occurs at such low energies in complexes of the type $\text{Fe}(\text{CO})_3\text{L}_2$ (L = N-donor ligand), the reaction is assumed to take place from the lowest ^3LF state after direct intersystem crossing from the $^1\text{MLCT}$ state. In view of the above-mentioned analogy between the electronic structures of $[\text{Fe}(\text{CO})_3(\text{R-DAB})]$ and the $\text{Fe}(\text{CO})_2(\text{L})$ fragments of the complexes under study, a similar process is assumed to occur for the binu-

clear complexes. The rates of these photosubstitution reactions do not depend on the cone angle of the phosphine ligand used, which indicates a dissociative pathway.

It is not yet clear whether the primary photoprocess is release of CO or breaking of a metal-nitrogen bond. According to our most recent results on the closely analogous $[\text{Fe}(\text{CO})_3(\text{R-DAB})]$ complexes, both reactions may occur and lead to the formation of the same photoproduct in which a carbonyl ligand is substituted by a nucleophile.⁴⁰

II. $[\text{Fe}_2(\text{CO})_6(\text{L})]$ (L = R-PyCa, R-DAB). In these complexes, which have the structure shown in Figure 1b, the ligand L is $\sigma\text{-N}, \mu\text{-N}', \eta^2\text{-CN}'$ (6e) bonded to both metal atoms. This change of coordination with respect to the bpy and phen ligands has a dramatic influence on the absorption spectrum. The intensive MLCT band has disappeared, and only a weak shoulder has remained in the visible region.

$[\text{Fe}_2(\text{CO})_6(\text{R-PyCa})]$ (R = *p*-Tol, *c*-Hex). Irradiation of these complexes (I) with the 488-nm line of an argon ion laser in 2-MeTHF (S) at 133 K (just above the glass point of this solvent) leads to the formation of $[\text{Fe}_2(\text{CO})_6(\text{R-PyCa})(\text{S})]$ (II) according to the reaction shown in Scheme I. The formation of II, in which the R-PyCa ligand is $\sigma, \sigma\text{-N}, \text{N}'$ (4e) coordinated to one of the iron atoms, is evident from the appearance of a strong MLCT band at 600 nm and from the near coincidence of its CO stretching frequencies with those of the corresponding photoproducts $[\text{Fe}_2(\text{CO})_6(\text{L})(\text{S})]$ (L = bpy, phen) (Table I). The two bands at 1771 and 1739 cm^{-1} belong to the two symmetrically bridging carbonyls that are absent in the parent compound. Figure 10 shows the CO stretching

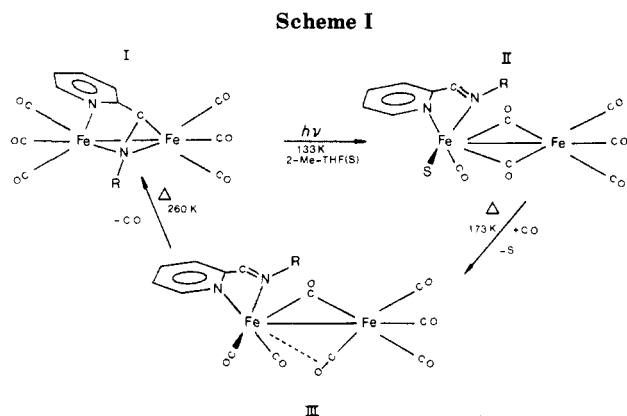
(41) Bénard, M.; Dedieu, A.; Nakamura, S. *Nouv. J. Chim.* 1984, 8, 149.

(42) Staal, L. H.; Stufkens, D. J.; Terpstra, A. *Inorg. Chim. Acta* 1979, 34, 97.

(43) Cromer, D. T.; Mann, J. B. *Acta Crystallogr., Sect. A: Cryst. Phys., Diffr., Theor. Gen. Crystallogr.* 1968, A24, 321.

(44) Stewart, J. M. "The X-Ray 76 System"; Technical Report Tr44, 1976; Computer Science Center, University of Maryland, College Park, MD.

(45) Walker, W.; Stuart, D. *Acta Crystallogr., Sect. A: Found. Crystallogr.* 1983, A39, 158.



region of the IR spectra of $[\text{Fe}_2(\text{CO})_6(\text{c-Hex-PyCa})]$ and of the photoproduct $[\text{Fe}_2(\text{CO})_6(\text{c-Hex-PyCa})(\text{S})]$ at 133 K. At room temperature complexes II show a complete back-reaction to the parent compound. When the temperature is raised to 173 K in the presence of added CO, the coordinated solvent molecule S is replaced by CO with formation of $[\text{Fe}_2(\text{CO})_7(\text{R-PyCa})]$ (III). In Figure 11 the electronic absorption spectra in the visible region of $[\text{Fe}_2(\text{CO})_6(p\text{-Tol-PyCa})]$ and $[\text{Fe}_2(\text{CO})_7(p\text{-Tol-PyCa})]$ are compared. The latter complex possesses an intensive MLCT band at 574 nm at 173 K. The position of this band strongly depends on the solution temperature. This so-called thermochromic effect is a characteristic feature of MLCT transitions.^{1,42} Complexes III are isostructural with the corresponding bpy and phen ones, which show within a few wavenumbers the same carbonyl stretching frequencies (Table I). Contrary to complexes II, complexes III possess a bent symmetrically bridging carbonyl ligand and a (nearly) symmetrically bridging carbonyl. Complexes III are stable up to 260 K. Above this temperature they react back to the parent compound I. Since the binuclear structure is retained and no CO is released during the photochemical conversion of I into II, the primary photoprocess is assumed to be the breaking of the $\eta^2\text{-CN}'$ bond between the R-PyCa ligand and one of the iron atoms.

$[\text{Fe}_2(\text{CO})_6(\text{R-DAB})]$ ($\text{R} = p\text{-Tol}, i\text{-Pr}, c\text{-Hex}, t\text{-Bu}$). Irradiation of these complexes with the 488-nm line of an argon ion laser in 2-MeTHF at 133 K leads to the formation of $[\text{Fe}_2(\text{CO})_5(\text{R-DAB})(\text{S})_2]$ compounds as evidenced by the formation of free CO which is not the result of decomposition because the reactions proceed with the occurrence of isosbestic points. At the same time there is a change of coordination of the R-DAB ligand from $\sigma\text{-N}, \mu\text{-N}'$, $\eta^2\text{-CN}'$ (6e) to $\sigma, \sigma\text{-N}, \text{N}'$ (4e) coordination giving rise to the appearance of a strong MLCT band at about 500 nm. From these results it cannot be concluded what the structure of these photoproducts is. The IR frequencies in the carbonyl stretching region and the maxima of the MLCT bands are also collected in Table I.

Acknowledgment. H. P. Gijben is thanked for preparing several of the complexes, A. Terpstra is thanked for his technical assistance, and Th. L. Snoeck is thanked for his help with the rR measurements. Finally P. van

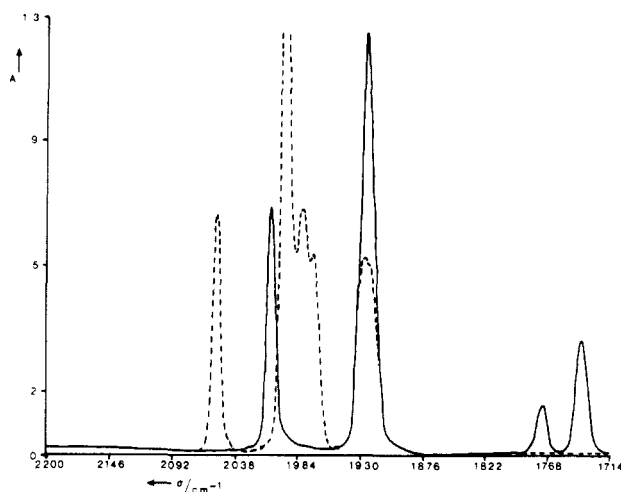


Figure 10. IR spectra of $[\text{Fe}_2(\text{CO})_6(\text{c-Hex-PyCa})]$ (dashed) and $[\text{Fe}_2(\text{CO})_6(\text{c-Hex-PyCa})(\text{S})]$ (drawn) in the CO-stretching region at 133 K in 2-MeTHF.

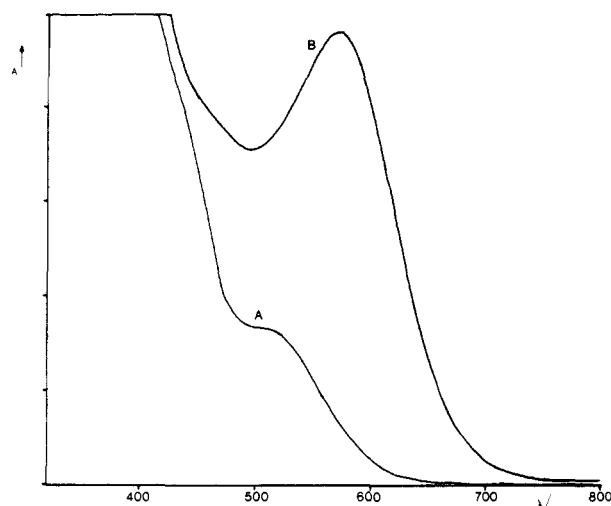


Figure 11. The electronic absorption spectra of $[\text{Fe}_2(\text{CO})_6(p\text{-Tol-PyCa})]$ (A) and $[\text{Fe}_2(\text{CO})_7(p\text{-Tol-PyCa})]$ (B) in 2-MeTHF at 173 K.

Haperen and I. Calonaci are thanked for performing some low-temperature photochemical experiments.

Registry No. $[\text{Fe}_2(\text{CO})_6(p\text{-Tol-PyCa})]$, 108023-09-2; $[\text{Fe}_2(\text{CO})_6(c\text{-Hex-PyCa})]$, 108023-07-0; $[\text{Fe}_2(\text{CO})_6(i\text{-Pr-DAB})]$, 74552-74-2; $[\text{Fe}_2(\text{CO})_6(p\text{-Tol-DAB})]$, 74552-76-4; $[\text{Fe}_2(\text{CO})_6(c\text{-Hex-DAB})]$, 65059-34-9; $[\text{Fe}_2(\text{CO})_6(t\text{-Bu-DAB})]$, 65045-67-2; $[\text{Fe}_2(\text{CO})_7(\text{bpy})]$, 52701-29-8; $[\text{Fe}_2(\text{CO})_7(\text{phen})]$, 87890-13-9; $[\text{Fe}_2(\text{CO})_7(p\text{-Tol-PyCa})]$, 108796-71-0; $[\text{Fe}_2(\text{CO})_7(c\text{-Hex-PyCa})]$, 108796-72-1; $[\text{Fe}_2(\text{CO})_6(\text{bpy})(2\text{-MeTHF})]$, 108796-73-2; $[\text{Fe}_2(\text{CO})_6(\text{phen})(2\text{-MeTHF})]$, 108796-74-3; $[\text{Fe}_2(\text{CO})_6(p\text{-Tol-PyCa})(2\text{-MeTHF})]$, 108796-75-4; $[\text{Fe}_2(\text{CO})_6(c\text{-Hex-PyCa})(2\text{-MeTHF})]$, 108796-76-5; $[\text{Fe}_2(\text{CO})_6(\text{bpy})(P(n\text{-Bu})_3)]$, 108796-77-6; $[\text{Fe}_2(\text{CO})_6(\text{bpy})(P(c\text{-Hex})_3)]$, 108796-78-7; $[\text{Fe}_2(\text{CO})_6(\text{bpy})(P(\text{Ph})_3)]$, 108796-79-8; $[\text{Fe}_2(\text{CO})_6(\text{bpy})(P(\text{OMe})_3)]$, 108796-80-1; $[\text{Fe}_2(\text{CO})_6(\text{bpy})(P(\text{OPh})_3)]$, 108796-81-2; $[\text{Fe}_2(\text{CO})_6(\text{bpy})(\text{py})]$, 108796-82-3; $[\text{Fe}_2(\text{CO})_6(\text{bpy})(n\text{-propylamine})]$, 108796-83-4; $[\text{Fe}_2(\text{CO})_6(\text{bpy})(\text{CH}_3\text{C}\equiv\text{N})]$, 108796-84-5; $[\text{Fe}_2(\text{CO})_6(\text{phen})(P(n\text{-Bu})_3)]$, 108796-85-6; $[\text{Fe}_2(\text{CO})_6(\text{phen})(P(\text{Ph})_3)]$, 108796-86-7; $[\text{Fe}_2(\text{CO})_6(\text{phen})(P(\text{OPh})_3)]$, 108796-87-8; Fe, 7439-89-6.